

ORGAN AND EFFECTIVE DOSE EVALUATION IN DIAGNOSTIC RADIOLOGY BASED ON IN-PHANTOM DOSE MEASUREMENTS WITH NOVEL PHOTODIODE-DOSEMETERS

Chiyo Kawaura*, Takahiko Aoyama, Shuji Koyama, Masataka Achiwa¹ and Masaki Mori¹
School of Health Sciences, Nagoya University, Daikominami, Higashi-ku, Nagoya 461-8673, Japan
¹Division of Radiology, Nagoya University Hospital, Tsurumai-chou, Showa-ku, Nagoya 466-8560, Japan

Received May 17 2005, revised November 7 2005, accepted November 16 2005

Organ and the effective doses of patients undergoing clinical X ray examinations of chest and abdomen were evaluated with an anthropomorphic phantom and a new dosimetry system. The system was comprised of 34 pin photodiode dosimeters placed in/on particular tissues or organs of the anthropomorphic phantom, where the tissues and organs are defined by the International Commission on Radiological Protection (ICRP) to estimate the effective doses. Dosimeter signals were acquired on a personal computer directly, and converted into absorbed doses, from which the organ and the effective doses were evaluated on the computer. Our study showed that organ doses ranged from <0.01 to 0.72 mGy in routine X-ray radiography of chest and of abdomen and from 0.07 to 55.91 mGy in routine computed tomography (CT) examinations with current multi-slice CT scanners. The effective dose observed in the chest CT examination was approximately 300 times higher than that in chest radiography.

INTRODUCTION

Recent advances in clinical X-ray technology have made X-ray-based diagnostic procedures so simple that the frequency of radiological examinations tends to increase every year⁽¹⁾. Unlike occupational exposure, medical exposure does not have a radiation dose limit though it has reference doses. The reasons are that the advantage of the use of radiation outweigh the disadvantages for the patients, and the dose level by medical exposure is usually lower than the level that causes any deterministic effect. However, the low dose level does not always mean that it is harmless. In a recent study by Berrington and Darby, it was estimated that the cancer risk for Japanese people by diagnostic X rays was about three times higher than that for the people of European and American countries⁽²⁾, which increased social concern on the effect of medical exposure to our health. Although physicians and co-workers are the few who understand the dose level for each X ray examination, it would be preferable to know the level to which unnecessarily large exposure doses could be reduced.

The quantity effective dose equivalent was introduced by the International Commission on Radiological Protection (ICRP) in 1977 (ICRP Publication 26)⁽³⁾ and the United Nations Scientific Committee on the Effects of Atomic Radiation (UNSCEAR)⁽⁴⁾ has adopted the quantity effective dose equivalent in 1982 as being the most appropriate indicator of

patient risk by medical exposure. In 1990, the ICRP established that patient exposure from diagnostic X rays should be denoted by organ dose and the effective dose where the latter was calculated from the dose values for various organs⁽⁵⁾. It is, however, difficult to estimate medical exposure to patients according to organ and effective doses. Since the evaluation of organ doses requires some complicated manipulations or calculations, it is often regarded as a troublesome job in medical facilities.

The measurements of organ doses have been carried out by thermoluminescent dosimeters (TLDs) implanted in tissue and organ positions within an anthropomorphic phantom consisting of tissue equivalent materials^(6–11). Some representative measurements of medical exposure in Japan were carried out by Maruyama and Nishizawa *et al.*^(8–11) in 1991–1996. Although their results were accepted in the UNSCEAR 2000 report⁽⁴⁾, available data on exposure doses by recent radiography are quite few in Japan. Another method of estimating organ and the effective doses is the Monte Carlo simulation of photon interactions within a simplified mathematical model of the human body^(12–14). Calculated dose values, however, should be verified by examinations using anthropomorphic or cylindrical phantoms and the same exposure conditions as the calculation⁽¹⁴⁾. Moreover, TLD-based in-phantom dosimetry and the Monte Carlo simulation are laborious and/or time-consuming.

In recent years a metal-oxide-semiconductor field effect transistor (MOSFET) dosimeter was devised as an alternative to TLDs for the measurement of

*Corresponding author: kawaura@met.nagoya-u.ac.jp

entrance surface dose⁽¹⁵⁾ and of organ dose⁽¹⁶⁾ in diagnostic radiology. The sensitivity of the MOSFET dosimeter, however, was not high enough with a measurable dose of >1.5 mGy; also, these dosimeters had a finite lifetime of 6 months and a maximum accumulated dose of the order of 7 Gy after which the dosimeters could no longer be used⁽¹⁵⁾. In order to break present state of the art, we devised a new dosimetry system using pin silicon photodiode X-ray dosimeters installed in an anthropomorphic phantom⁽¹⁷⁾. In the previous study with a thoracic phantom, we compared the computed tomography dose index (CTDI) measured with a standard computed tomography (CT) ion chamber with the integrated dose value calculated from a dose profile measured with the pin photodiode dosimeter, and made it clear that integrated dose values with the photodiode dosimeter agreed with the CTDI values from the CT ion chamber within 10%⁽¹⁷⁾. These results suggested that the pin photodiode dosimeter would be useful for in-phantom dose measurement by medical exposure. In the present paper, we describe organ and the effective dose evaluation in X-ray radiography and CT examinations using the new dosimetry system which employs the photodiode dosimeters embedded in an anthropomorphic phantom and computer data acquisition and processing.

MATERIALS AND METHODS

In-phantom dosimetry system

Pin silicon photodiodes, Hamamatsu S2506-04 [Hamamatsu Photonics, K. K., Japan, <http://jp.hamamatsu.com/products/node.do?dir=/>], were used as the detector part of the dosimeter. The photodiode with a relatively large sensitive area of 2.8×2.8 mm² is low in price of about 2 US dollars in Japan and moulded out of black resin, 2.7 mm thick, for infrared spectral response. Since the sensitivity of the single photodiode to diagnostic X rays differed by incident direction of X rays between front and back as shown in Figure 1, two photodiodes were glued together back-to-back with epoxy cement, and were used as a single detector with parallel connection to obtain isotropic sensitivity to incident X rays⁽¹⁷⁾.

Dose calibrations were performed against a Radcal 1015 dosimeter with a 6 cm³ ion chamber attached, which was placed adjacent to a photodiode dosimeter, a few centimetres apart, at the same distance from the X-ray tube in an irradiation field. The ion chamber dosimeter is a tertiary standard, calibrated at a laboratory of the Japan Quality Assurance Organization in April 2001, where dosimeter readings were calibrated to exposure dose values at nine points of effective or equivalent photon energies⁽¹⁸⁾ from 20 to 72 keV. Photodiode dosimeter readings

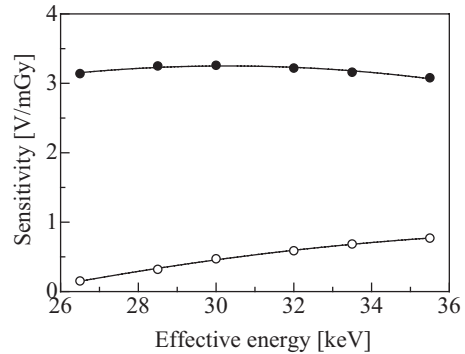


Figure 1. X-ray energy dependence of the sensitivity of a single photodiode, where the sensitivity is the output voltage per absorbed dose for soft tissue. Closed circles indicate sensitivities for front irradiation, and open circles for back irradiation of X rays.

thus calibrated to exposure dose were converted to absorbed dose in soft tissue by using mass energy-absorption coefficient for soft tissue⁽¹⁹⁾ at each effective energy. X-ray energy dependence of the sensitivity of the dosimeters was found to be approximately flat within 5% in an effective energy range between 27 and 50 keV, but decreased at a rate of 9.5%/10 keV with increasing energy between 50 and 70 keV⁽¹⁷⁾.

The dosimeters were installed within an anthropomorphic phantom at the positions of various tissues or organs assigned in the ICRP's definition of the effective dose, where the phantom, which modelled the standard Japanese adult man, 170 cm tall and 60 kg in weight, was manufactured by Kyoto Kagaku, (Kyoto Kagaku Co. Ltd., Japan, <http://www.kyotokagaku.com/>). The phantom, which is that of the torso, was constructed with three types of tissue substitutes, viz. Tough Water (WE-211), Tough Bone (BE-303) and Tough Lung (LP-430)⁽²⁰⁾, corresponding to soft tissue, skeleton and lung, respectively. To evaluate organ dose to the breast, the left breast made up with MixDp⁽²¹⁾ was attached to the phantom. The phantom was sliced into 15 pieces each of thickness 50 mm, and each slice was drilled with a hole of diameter of 11 mm to enable insertion of the dosimeters in the position of each organ as illustrated in Figure 2, where organ positions were decided from the roentgenogram of the phantom and an anatomical chart. These drilled holes were filled with tissue equivalent epoxy resin after dosimeters were set in the holes. Carbon fibre cables used to connect dosimeters and readout electronics were led to the back of the phantom through a groove made on the flat surface of the same phantom section. Positions of 32 dosimeters implanted within the phantom are shown in Figure 3 and Table 1 by numbering the dosimeters.

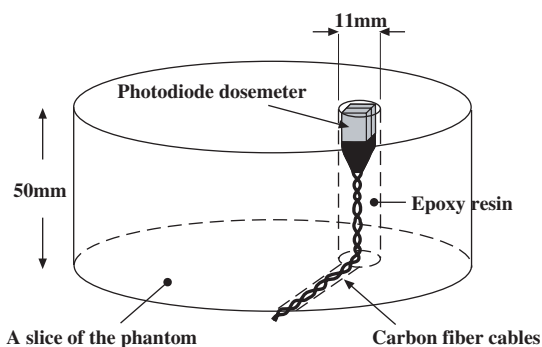


Figure 2. Shema of the setting of the photodiode dosemeter in a slice of the phantom, where the photodiode was connected to a pair of twisted carbon-fibre cables.

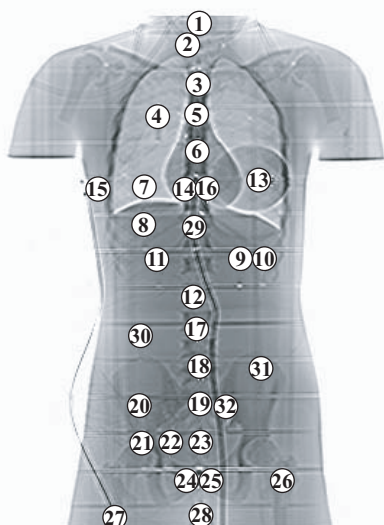


Figure 3. Roentgenogram of a dosemeter implanted in an anthropomorphic phantom, where dosemeter positions are numbered in the roentgenogram

Since dosemeter materials, such as silicon wafer, thin metal-plate backing and lead metals, are slightly different from phantom materials the placement of the dosemeter in the phantom might affect dose values of another dosemeter placed in the same slice of the phantom owing to shadow effect or shielding of X rays. The shadow effect would be at the maximum when direct X rays exactly pass two or more dosemeters and the distance of the dosemeters is small in the phantom. Dose difference was measured at the rectum position (dosemeter no. 24) when the dosimeter at the bladder position (dosemeter no. 25), only 4 cm away from the

Table 1. The location of 34 photodiode dosemeters in the phantom, where the number of the dosemeter corresponds to that in Figure 3.

Organ name	The position of numbered dosemeters	w_T
Gonads	(22) (Ovary) (28) (Testes)	0.20
Red bone marrow	(1) (Cervical vertebrae) (3) (Sternum, Clavicles) (6) (Thoracic vertebrae, Scapulae, Rib) (17) (Lumbar vertebrae) (19) (Sacrum) (20) (Os coxae) (21) (Os coxae) (26) (Femur)	0.12
Colon	(12) (Transverse colon) (24) (Rectum) (30) (Ascending colon) (31) (Descending colon) (32) (Sigmoid)	0.12
Lung	(4) (7)	0.12
Stomach	(9)	0.12
Bladder	(25)	0.05
Breast	(13)	0.05
Liver	(8) (11)	0.05
Oesophagus	(5) (29)	0.05
Thyroid	(2)	0.05
Skin	(33) ^(a) (34) ^(a)	0.01
Bone surface	(3) (Sternum, Clavicles) (6) (Thoracic vertebrae, Scapulae) (14) (Rib) (15) (Rib) (16) (Rib) (17) (Lumbar vertebrae) (19) (Sacrum) (20) (Os coxae) (21) (Os coxae) (27) (Femur)	0.01
Remaining organs	(3) (Thymus) (10) (Spleen) (11) (Adrenals, Kidney) (12) (Pancreas) (18) (Small intestine) (23) (Uterus)	0.05

^(a)Extra dosemeters externally attached to the surface of the phantom

Organ doses of 13 tissues and organs were assessed to estimate the effective dose by using the tissue weighting factor w_T . The parentheses indicate subdivided organs in which the dosemeters were implanted

rectum position, was replaced by the phantom material, Tough Water. When X rays were irradiated from the anterior–posterior (AP) direction dose values at the rectum position were found to increase by 8% at the maximum in the effective energy range of X rays used. This resulted in the underestimation of the colon dose averaged in the whole of the colon by 1.2% in the hip joint radiography. The difference, however, could be completely negligible when compared with total

accuracy of ~10% of the present dose measurement. For CT examinations it would be clear that the shadowing effect is negligible since X rays pass two or more dosimeter positions in the same phantom slice only in a moment.

Calculation of organ doses

Output voltage signals generated from the 32 photodiode dosimeters were read out with a personal computer through AD converters, and each signal was converted to the absorbed dose for soft tissue by using the 'conversion factor,' in mGy/V, at the effective energy of X rays used, where the conversion factor is the reciprocal of the dosimeter sensitivity—see Figure 1. Conversion factors for the 32 dosimeters were separately determined by using the factor for a standard dosimeter—one of the 32 dosimeters—calibrated for an effective energy range between 23 and 72 keV and the ratios of the factor for each dosimeter to that of the standard, where the ratios were measured at an effective energy of 30 keV. This series of data processing was performed using an original program loaded in the computer. The minimum detectable organ dose could be estimated using a sensitivity of ~0.48 V mGy⁻¹ and a quantum error of the ADC used of 2.5 mV to be 0.01 mGy with 50% uncertainty⁽¹⁷⁾.

For small organs like the thyroid and gonads, absorbed dose values obtained from the dosimeter installed in the centroid of the organ were adopted as the organ dose. For organs with large volume such as the lung, liver and colon, 2–5 dosimeters were set at each centroid of the organ subdivided equally, and the mean dose value was regarded as the organ dose. Organ dose for colon, D_{colon} , was calculated according to ICRP Publication 67⁽²²⁾ from the formula

$$D_{\text{colon}} = 0.57D_{\text{ULI}} + 0.43D_{\text{LLI}}, \quad (1)$$

where D_{ULI} and D_{LLI} are the absorbed doses in walls of the upper large intestine (ULI) and lower large intestine (LLI), respectively. D_{ULI} is the average dose of the ascending and transverse colons, and D_{LLI} is that of the descending colon, sigmoid and rectum.

Dose for red bone marrow, $D_{\text{bone marrow}}$, was evaluated from the equation

$$D_{\text{bone marrow}} = \sum_i D_{\text{abs},i} \cdot A_i, \quad (2)$$

where $D_{\text{abs},i}$ is the absorbed dose for soft tissue at each measuring point in various bone tissues. This is because mass energy-absorption coefficients for red bone marrow coincided with those for soft tissue within 5% in diagnostic X-ray energy of >30 keV⁽²³⁾. A_i is the weight fraction of each red bone marrow, the values of which were shown in Table 2. The weight fraction, i.e. contribution of individual red

Table 2. Weight fractions of red bone marrow and mineralised bone listed in ICRP Publication 70.

Bone name	Weight fractions	
	Red bone marrow (A_i)	Mineralised bone (M_i)
Scapulae	0.029	0.031
Clavicles	0.008	0.012
Sternum	0.030	0.005
Ribs	0.152	0.073
Cervical vertebrae	0.037	—
Thoracic vertebrae	0.153	0.056
Lumbar vertebrae	0.117	0.035
Sacrum	0.094	0.020
Os coxae	0.195	0.084
Femur	0.074	0.186

The weight fractions of red bone marrow are values for humans 25 years old, and those of mineralised bone are for Japanese adult male

bone marrow in total weight, could be quoted from ICRP Publication 70⁽²⁴⁾. Since the phantom used is torso, the absorbed doses of the limbs and the skull were not included in the calculated value of $D_{\text{bone marrow}}$.

Dose for the bone surface, $D_{\text{bone surface}}$, was evaluated from the equation

$$D_{\text{bone surface}} = \left\{ \sum_i D_{\text{abs},i} \cdot M_i \right\} \times \left\{ (\mu_{\text{en}}/\rho)_{\text{bone, cortical}} / (\mu_{\text{en}}/\rho)_{\text{tissue, soft}} \right\}, \quad (3)$$

where M_i is the weight fraction of mineralised bone as indicated in Table 2, and $(\mu_{\text{en}}/\rho)_{\text{bone, cortical}}$ and $(\mu_{\text{en}}/\rho)_{\text{tissue, soft}}$ are the mass energy-absorption coefficients for cortical bone and soft tissue, respectively⁽¹⁹⁾. Because dose measurement for the bone surface was technically difficult, the same dose values as those in Equation (2), $D_{\text{abs},i}$, were used for the evaluation of the bone surface dose.

Dose for the breast, D_{breast} , was evaluated from the equation

$$D_{\text{breast}} = D_{\text{abs},b} \times \left\{ (\mu_{\text{en}}/\rho)_{\text{breast}} / (\mu_{\text{en}}/\rho)_{\text{tissue, soft}} \right\}, \quad (4)$$

where $D_{\text{abs},b}$ is absorbed dose for soft tissue at the measuring point in the breast, and $(\mu_{\text{en}}/\rho)_{\text{breast}}$ is mass energy-absorption coefficient for the breast⁽¹⁹⁾.

For the evaluation of skin dose absorbed doses at the entrance and the exit of X rays were measured by using two extra dosimeters—see Table 1—attached

to the surface of the phantom. Dose calibration for these dosimeters was performed separately for the effective energy range described above. Average dose values of the two dosimeters were multiplied by the ratio of the irradiated area to the gross surface area of the phantom to calculate organ dose for the skin. The gross surface area of the phantom having head, arms and legs was estimated to be 1.60 m².

Evaluation of the effective dose

Evaluation formula of the effective dose is given by ICRP Publication 60⁽⁵⁾ in the expression

$$E = \sum_T w_T \cdot H_T, \tag{5}$$

where w_T is the tissue weighting factor recommended by ICRP Publication 60⁽⁵⁾ and H_T is the equivalent dose of each organ dose multiplied by the radiation weighting factor of unity for X rays. The weighting factors of the specified thirteen organs are given in ICRP Publication 60⁽⁵⁾, which are shown in Table 1. The remaining organs are subdivided into 9 organs, which are the adrenals, brain, small intestine, kidney, muscle, pancreas, spleen, thymus and uterus⁽⁵⁾. Brain dose, not measured because of the use of the headless phantom, was assumed to be zero since negligibly small values would be expected except for head examinations. Muscle was excluded from the remaining organs since it was difficult to measure the absorbed dose of the muscle extending to the

whole body. The uterus was included in the remaining organs for females alone, and not for males. For the gonads, the testes and ovary doses were used for male and female, respectively.

Technical parameters and X-ray generators

The organ and the effective doses for patients were evaluated for the typical X ray examinations of chest and abdomen in X ray CT and other diagnostic radiology. Four-channel multi-slice CT scanner (MSCT), Toshiba Aquilion, was used as the CT scanner. A three-phase 12-pulse X-ray generator, Toshiba KXO-850, was used in radiography. Technical parameters for MSCT and radiography for routine examinations that have been used in Nagoya University hospital are shown in Tables 4 and 5, respectively.

RESULTS AND DISCUSSIONS

Organ doses

For organs with large volume such as the colon, several dosimeters were placed in each segment, and the mean dose value was regarded as the organ dose. Measured values of each colon segment in CT examinations are noted in Table 3. It is seen from Table 3 that doses for the segments exposed to primary X rays show large values. The values of D_{ULI} and D_{LLI} were used to calculate colon dose—see Equation (1). Table 3 also shows absorbed doses

Table 3. Absorbed doses for each segment of the colon and for each part of the bone measured in various CT examinations, where the doses (mGy) are those for soft tissue.

	Chest	Chest–Abdomen	Abdomen–Pelvis	Pancreas	Liver
D_{abs}					
Segments of colon					
Ascending colon	2.68	17.23	39.90	21.39	30.86
Transverse colon	9.64	20.46	45.44	25.52	37.98
Descending colon	0.99	5.19	37.74	5.60	6.62
Sigmoid colon	0.44	1.64	39.85	1.93	2.15
Rectum	0.18	0.45	33.21	0.44	0.50
D_{ULI}	6.16	18.84	42.67	23.46	34.42
D_{LLI}	0.54	2.43	36.93	2.66	3.09
$D_{abs, i}$					
Bones					
Cervical vertebrae	6.90	3.71	0.62	0.18	0.50
Sternum	39.95	22.98	1.46	0.39	1.23
Thoracic vertebrae	32.62	17.90	6.72	1.39	5.38
Lumbar vertebrae	2.90	14.32	36.32	18.20	25.52
Sacrum	0.52	1.67	29.57	1.90	2.21
Os coxae	0.37	1.05	32.02	1.37	1.42
Femur	0.10	0.23	26.32	0.32	0.31

Colon doses were calculated from values of D_{ULI} and D_{LLI}

Table 4. Technical parameters and organ doses in various CT examinations for Toshiba Aquilion multi-slice CT scanner, where the parameters are those used in the routine in Nagoya University hospital.

	Chest	Chest–Abdomen	Abdomen–Pelvis	Pancreas	Liver
Technical parameters					
Tube voltage (kV)	120	120	120	120	120
Tube current (mA)	350	300	400	300	350
Exposure time (s/rot.)	0.5	0.5	0.5	0.5	0.5
Effective (mA s/rot.)	175	150	200	150	175
Beam width	4 mm × 4	2 mm × 4	5 mm × 4	1 mm × 4	3 mm × 4
Helical pitch	3.0	5.5	3.0	5.5	3.0
Scan area (mm)	300	407	405	154	180
Organ doses (mGy)					
Organs					
Testes	0.07	0.15	7.32	0.17	0.17
Ovary	0.22	0.68	37.92	0.81	0.88
Red bone marrow	13.14	9.04	17.54	3.09	5.36
Colon	3.74	11.79	40.21	14.51	20.95
Lung	37.44	19.73	15.95	2.02	11.81
Stomach	32.35	22.08	40.65	24.58	40.69
Bladder	0.12	0.33	39.77	0.39	0.43
Breast	23.91	11.37	21.80	1.29	7.49
Liver	30.24	18.48	35.81	14.94	32.78
Oesophagus	33.50	18.81	19.45	7.42	17.80
Thyroid	48.76	27.91	0.88	0.25	0.73
Skin	6.05	4.05	7.58	1.58	2.98
Bone surface	35.40	22.23	55.91	6.33	18.71
Remaining (Male)	19.60	14.96	29.03	13.65	21.60
Remaining (Female)	17.18	13.18	29.55	12.04	19.01
Uterus	0.21	0.72	33.18	0.81	0.94

The gonad is classified to the testes for male and the ovary for female

measured for each part of the bone. These values were multiplied by the weight fraction of each red bone marrow as shown in Table 2 to evaluate the organ doses for red bone marrow—see Equation (2). In the same way, the organ doses for bone surface were also evaluated using Equation (3)—i.e. the dose for each part of the bone multiplied by the weight fraction and the ratio of mass energy-absorption coefficients for cortical bone and for soft tissue.

The organ doses obtained in CT examinations and X-ray radiography were summarised in Tables 4 and 5, respectively. The organ doses for organs exposed to primary X rays indicated large values, several tens of mGy in CT examinations, compared to those not directly exposed. Lung, esophagus and stomach doses, therefore, were comparatively high in chest and chest–abdomen CT examinations. On the other hand, doses for the colon, stomach, bladder and liver were higher in the abdomen–pelvis CT examination. In our study, the thyroid dose of 49 mGy was the highest in the chest CT examination. This was caused by clinical experience that the thyroid was usually included in the scan area in the chest CT examination to detect thyroid disease. Since

medical opinions about disease largely differ depending on the physician, it is necessary to pay attention to the thyroid dose when the thyroid is included in the scan area. In the abdomen–pelvis CT examination, the bone surface dose of 56 mGy was the highest, which could be explained by the abundant mineralised bone in the pelvis portion. Since the nominal fatality coefficient⁽⁵⁾ for radiation induced bone cancer is $5.0 \times 10^{-4} \text{ Sv}^{-1}$, fatal cancer induced probability for bone surface was 3.0×10^{-5} , which is negligibly small. On the contrary, stomach and colon doses were comparatively high in abdomen–pelvis CT examination, i.e. 41 and 40 mGy, respectively. Since nominal fatality coefficients of these organs are higher than those of other organs, i.e. $1.1 \times 10^{-2} \text{ Sv}^{-1}$ and $8.5 \times 10^{-3} \text{ Sv}^{-1}$ for stomach and colon respectively, the fatal cancer induced probability calculated was approximately ten times higher than that for the bone surface, i.e. 4.0×10^{-4} and 3.0×10^{-4} for stomach and colon cancer, respectively.

Generally, in medical exposure, organs for which patient worries are the gonads, because the gonads are believed to be much more sensitive to radiation

Table 5. Technical parameters and organ doses in X-ray radiography, where the parameters are those used in the routine in Nagoya University hospital.

	Chest (PA)	Chest (LAT)	Thoracic vertebrae (AP)	Thoracic vertebrae (LAT)	Abdomen (AP)	Hip joint (AP)	Pelvis (AP)	Lumbar vertebrae (AP)	Lumbar vertebrae (LAT)
Technical parameters									
Tube voltage (kV)	100	130	72	70	72	72	72	72	84
Tube current (mA)	320	250	200	200	200	200	200	200	200
Exposure time (s)	0.02	0.025	0.12	0.12	0.08	0.08	0.08	0.12	0.18
Effective (mA s)	6.40	6.25	24.00	24.00	16.00	16.00	16.00	24.00	36.00
FID (cm)	200	200	115	115	115	115	115	115	115
Organ doses (mGy)									
Organs									
Testes	<0.01	<0.01	0.01	0.02	0.02	0.58	0.65	0.01	0.03
Ovary	<0.01	0.01	<0.01	0.02	0.37	0.50	0.49	0.15	0.33
Red bone marrow	0.06	0.05	0.09	0.04	0.08	0.11	0.11	0.08	0.23
Colon	0.02	0.04	0.04	0.05	0.30	0.20	0.22	0.40	0.44
Lung	0.16	0.29	0.46	0.31	0.02	0.03	<0.01	<0.01	0.02
Stomach	0.06	0.10	0.72	0.06	0.43	0.05	0.02	0.51	0.03
Bladder	<0.01	0.01	0.01	0.02	0.10	0.44	0.45	0.03	0.12
Breast	0.04	0.26	0.57	0.02	0.04	0.01	0.01	0.02	0.01
Liver	0.12	0.37	0.27	0.40	0.16	0.04	0.01	0.11	0.05
Oesophagus	0.11	0.16	0.33	0.14	0.07	0.03	<0.01	0.02	0.02
Thyroid	0.08	0.29	0.11	0.04	<0.01	0.04	<0.01	<0.01	0.02
Skin	0.02	0.05	0.05	0.06	0.06	0.07	0.06	0.04	0.10
Bone surface	0.18	0.22	0.45	0.36	0.24	0.56	0.53	0.20	0.70
Remaining (Male)	0.07	0.12	0.21	0.12	0.17	0.10	0.08	0.24	0.05
Remaining (Female)	0.06	0.11	0.19	0.11	0.17	0.12	0.10	0.22	0.07
Uterus	<0.01	<0.01	<0.01	0.01	0.17	0.26	0.21	0.11	0.20

Incident directions of X-rays are posterior–anterior (PA), anterior–posterior (AP) and lateral (LAT). FID means focus-to-image receptor distance

than other organs. The highest gonad dose obtained in our study was 38 mGy for the ovary in the abdomen–pelvis CT examination (Table 4). In the case of the testes, the threshold of temporary sterility is 0.15 Sv and that of permanent sterility is 3.5–6.0 Sv⁽⁵⁾. On the other hand the threshold of permanent sterility for the ovary is 2.5–6.0 Sv⁽⁵⁾. The risks of temporary and permanent sterility by gonadal exposure, therefore, are negligibly small because gonad doses are far lower than these thresholds. In the abdomen–pelvis CT examination the uterus dose was also high with a value of 33 mGy. Radiation-induced malformation or mental retardation of the fetus may occur depending on the duration of radiation exposure after pregnancy and absorbed dose for the fetus above the threshold of 100 mGy⁽⁵⁾. Since measured uterus doses were lower than the threshold value, it is not necessary for us to worry about deterministic effects like malformation or mental retardation of the fetus in the abdomen–pelvis CT examination. On the other hand, the probability of induced childhood cancer estimated from the uterus dose and the probability at

10 mGy of 0.06%⁽²⁵⁾ was 0.2%, the value which is of the same order as the ‘background’ cancer risk. We should, therefore, pay attention to the operation of the abdomen–pelvis CT examination for pregnant women.

Unlike CT examinations, radiography is known to deliver extremely low exposure doses. Table 5 shows organ doses observed in X-ray radiography of the trunk. Each value is seen to be low with values of <1.0 mGy with a maximum of 0.72 mGy for stomach dose in thoracic vertebrae AP examination. Gonad doses were comparatively high in the pelvis and hip joint examinations with testes and ovary doses of 0.65 and 0.49 mGy, and of 0.58 and 0.50 mGy, respectively. Because organ doses observed in X-ray radiography were extremely small, deterministic and probabilistic effects would be negligible in comparison with CT examinations. In fact, organ doses in the chest radiography posterior–anterior (PA) were more than two orders smaller than those in the chest CT examination. Considering the present state of radiological diagnosis where most examinations shift from X-ray

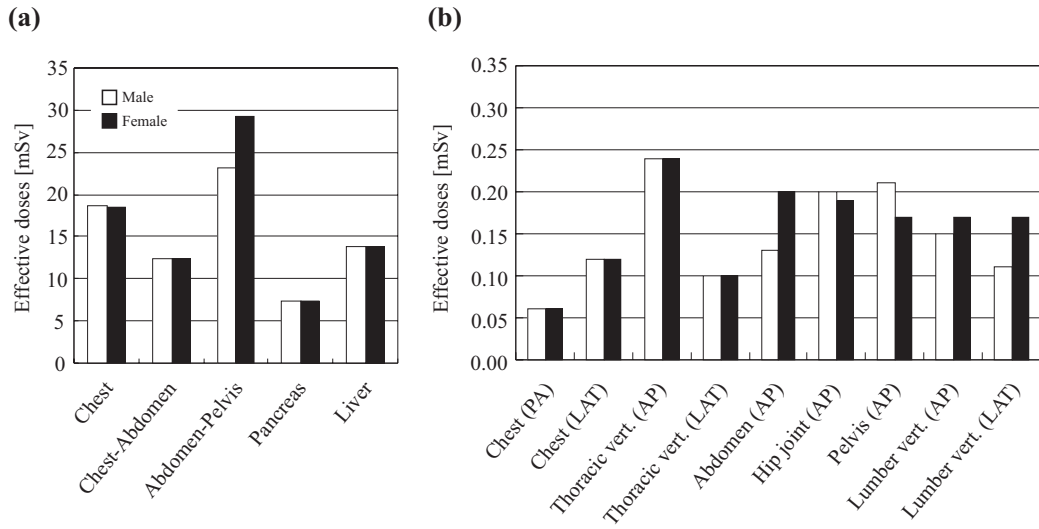


Figure 4. Effective doses observed in CT examinations (a) and X-ray radiography (b). White and black bars show the effective doses for male and female, respectively.

radiography to CT examinations, risk of medical exposure would increase.

Effective doses

Figure 4(a) shows effective doses obtained from various CT examinations. Effective dose for chest–abdomen CT examination was 12.4 mSv, for both male and female. On the other hand, effective doses for abdomen–pelvis CT examination were 23.2 and 29.3 mSv for male and female, respectively. From dose measurement using TLDs and Rando phantom, Nishizawa *et al.*⁽¹⁵⁾ found the effective doses for chest–abdomen CT examination to be 12.5 mSv for male and female, and those for abdomen–pelvis CT examination to be 23.4 mSv for male and 27.7 mSv for female for the same CT scanner and technical conditions as ours. Agreement of dose values was excellent with the difference being between 1 and 6%. In recent years, Cohnen *et al.*⁽⁷⁾ assessed the radiation exposure of patients in several standard protocols in multi-slice CT (MSCT) examinations. They compared the effective doses calculated using the weighted CTDI with those actually measured by using TLDs and Rando phantom, and reported that the effective doses in both methods agreed well. Their results for actual measurement were 7.5–12.9 mSv in the chest CT examination and 12.4–16.1 mSv in the abdomen CT examination. In the calculation based on the CTDI, effective doses were 6.4–14.2 mSv in the chest CT examination and 9.6–18.9 mSv in the abdomen CT examination. Our results in the chest and abdomen–pelvis CT examinations, which are equivalents to the chest and

Table 6. Comparison of the average effective dose for male and female in radiography obtained in the present study and the effective dose values listed in the UNSCEAR 2000 report as Japanese data.

Radiography	Effective dose (mSv)	
	Present study	UNSCEAR 2000
Chest (PA)	0.060	0.057
Chest (LAT)	0.120	—
Thoracic vertebrae (AP)	0.240	0.650
Thoracic vertebrae (LAT)	0.100	—
Abdomen (AP)	0.160	0.240
Hip joint (AP)	0.195	0.580
Pelvis (AP)	0.190	0.580
Lumbar vertebrae (AP)	0.160	1.450
Lumbar vertebrae (LAT)	0.140	—

abdomen CT examination measured by Cohnen *et al.*⁽⁷⁾, were both slightly higher than their results. Although scan areas which Cohnen *et al.*⁽⁷⁾ measured were roughly equivalent to ours, the technical parameters they used were different from those in our examinations. The differences of the two sets of results might be attributed to technical parameters used, the performance of CT scanners and partly to the phantom used.

On the other hand, effective doses for chest and abdomen radiography ranged from 0.06 to 0.24 mSv as seen in Figure 4(b) and Table 6. The effective dose in routine chest radiography was 0.06 mSv per examination, for both male and female. According to the UNSCEAR 2000 report⁽¹⁾, the effective dose in the

chest radiography in Japan was 0.057 mSv, which value agreed with our result. However, the effective dose in the UNSCEAR 2000 report⁽¹⁾ for the lumbar vertebrae (AP) examination was approximately ten times higher than that obtained in the present study as seen in Table 6, while the dose values for the thoracic vertebrae (AP) and hip joint (AP) examinations by UNSCEAR⁽¹⁾ were a few times higher. The differences between these dose values would be attributed to the differences in radiography techniques and the X-ray generator used.

CONCLUSIONS

An organ dose measuring system using photodiode dosimeters installed within an anthropomorphic phantom was devised to assess the effect of medical exposure on patients undergoing various radiological examinations. By using a computer readout system, the organ and the effective doses delivered by X-ray irradiation could be rapidly evaluated. Effective dose values in CT examinations agreed well with the data of other researchers measured using TLDs and Rando phantom. However, the differences observed in effective doses of radiography examinations between our study and the UNSCEAR 2000 report amounted to several times. The effective dose obtained in chest CT examination was approximately 300 times higher than that in chest radiography. The present system, having the advantages of rapid and convenient data acquisition, could become a powerful tool for measuring organ doses of patients in various diagnostic X-ray examinations.

ACKNOWLEDGEMENT

This study was supported in part by a grant-in-aid for Scientific Research (No. 14580568) from the Ministry of Education, Culture, Sports, Science and Technology of Japan, which the authors greatly appreciate.

REFERENCES

1. United Nations Scientific Committee on the Effects of Atomic Radiation, Sources and Effects of Ionizing Radiation. *2000 Report to the General Assembly, with scientific annexes*. (NY: UNSCEAR) (2000).
2. Berrington de Gonzalez, A. and Darby, S. *Risk of cancer from diagnostic X-rays: estimates for the UK and 14 other countries*. *Lancet* **363**, 345–351 (2004).
3. International Commission on Radiological Protection. *Recommendations of the International Commission on Radiological Protection*. ICRP Publication 26. Ann ICRP **1**(3) (Oxford: Pergamon Press) (1977).
4. United Nations Scientific Committee on the Effects of Atomic Radiation. *Ionizing radiation: sources and biological effects*. UNSCEAR Report 1982. (NY: United Nations) (1982).

5. International Commission on Radiological Protection. *1990 Recommendations of the International Commission on Radiological Protection*. ICRP Publication 60. Ann. ICRP **21** (1–3) (Oxford: Pergamon Press) (1991).
6. Mini, R. L., Vock, P. Mury, R. and Schneeberger, P. P. *Radiation exposure of patients who undergo CT of the trunk*. *Radiology* **195**, 557–562 (1995).
7. Cohnen, M., Poll, L. J., Puettmann, C., Ewen, K., Saleh, A. and Modder, U. *Effective doses in standard protocols for multi-slice CT scanning*. *Eur. Radiol.* **13**, 1148–1153 (2003).
8. Nishizawa, K., Maruyama, T., Takayama, M., Okada, M., Hachiya, J. and Furuya, Y. *Determinations of organ doses and effective dose equivalents from computed tomographic examination*. *Br. J. Radiol.* **64**, 20–28 (1991).
9. Nishizawa, K., Maruyama, T., Takayama, M., Iwai, K. and Y. Furuya, Y. *Estimation of effective dose from CT examination*. *Nippon Acta Radiol.* **55**, 763–768 (1995).
10. Maruyama, T., Iwai, K., Nishizawa, K., Noda, Y. and Kumamoto, Y. *Organ or tissue doses, effective dose and collective effective dose from x-ray diagnosis, in Japan*. *Radioisotopes* **45**, 761–773 (1996).
11. Nishizawa, K., Matsumoto, M., Iwai, K., Tonari, A., Yoshida, T. and Takayama, M. *Dose evaluation and effective dose estimation from multi detector CT*. *Japan J. Med. Phys.* **22**, 152–158 (2002).
12. Zankl, M. *Methods for assessing organ doses using computational models*. *Radiat. Prot. Dosim.* **80**, 207–212 (1998).
13. McCollough C. H. and Schueler, B. A. *Calculation of effective dose*. *Med. Phys.* **27**, 828–837 (2000).
14. Caon, M., Bibbo, G. and Pattison, J. *A comparison of radiation dose measured in CT dosimetry phantoms with calculations using EGS4 and voxel-based computational models*. *Phys. Med. Biol.* **42**, 219–229 (1997).
15. Peet, D. J. and Pryor, M. D. *Evaluation of a MOSFET radiation sensor for the measurement of entrance surface dose in diagnostic radiology*. *Br. J. Radiol.* **72**, 562–568 (1999).
16. Sessions, J. B., Roshau, J. N., Tressler, M. A., Hintenlang, D. E., Arreola, M. M., Williams, J. L., Bouchet, L. G. and Bolch, W. E. *Comparison of point and average organ dose within an anthropomorphic physical phantom and a computational model of the newborn patient*. *Med. Phys.* **29**, 1080–1089 (2002).
17. Aoyama, T., Koyama, S. and Kawaura, C. *An in-phantom dosimetry system using pin silicon photodiode radiation sensors for measuring organ doses in x-ray CT and other diagnostic radiology*. *Med. Phys.* **29**, 1504–1510 (2002).
18. Attix, F. H. *Introduction to radiological physics and radiation dosimetry*. (New York: Wiley) pp. 226 (1986).
19. Hubbell, J. H. and Seltzer, S. M. *Tables of X-ray mass attenuation coefficients and mass energy-absorption coefficients 1 keV to 20 MeV for elements Z=1 to 92 and 48 additional substance of dosimetric interest*. Report No. NISTIR 5632 (National Institute of Standards and Technology, Gaithersburg, MD) (1995).
20. Kyoto Kagaku Co., Ltd. *Specifications of THRA1 therapy body phantom*. Kyoto (in Japanese).

21. Onai Y. and Kusumoto, G. *Trial production of a water-equivalent solid phantom material*. *Nippon Acta Radiol.* **19**, 1012–1016 (1959).
22. International Commission on Radiological Protection. *Age-dependent doses to members of the public from intake of radionuclides*. ICRP Publication 67. Ann. ICRP **23**(3–4) (Oxford: Pergamon Press) (1994).
23. International Commission on Radiation Unit and Measurements. *Photon, electron, proton and neutron interaction data for body tissues*. ICRU Report 46 (Bethesda, MD: ICRU) (1992).
24. International Commission on Radiological Protection. *Basic anatomical & physiological data for use in radiological protection: the skeleton*. ICRP Publication 70. Ann. ICRP **25**(2) (Oxford: Pergamon Press) (1995).
25. International Commission on Radiological Protection. *Pregnancy and medical radiation*. ICRP Publication 84. Ann. ICRP **31**(1) (Oxford: Pergamon Press) (2000).

